Available online at www.sciencedirect.com

ScienceDirect

Journal of Colloid and Interface Science 306 (2007) 205–215

JOURNAL OF Colloid and Interface Science

www.elsevier.com/locate/jcis

The influence of functionality on the adsorption of *p*-hydroxy benzoate and phthalate at the hematite–electrolyte interface

Manash R. Das, Sekh Mahiuddin *

Material Science Division, Regional Research Laboratory, Jorhat 785006, Assam, India

Received 3 July 2006; accepted 22 October 2006

Available online 26 October 2006

Abstract

Kinetics of adsorption of *p*-hydroxy benzoate and phthalate on hematite–electrolyte interface were investigated at a constant ionic strength, $I = 5 \times 10^{-4}$ mol dm^{-3}, pH 5 and at three different temperatures. The state of equilibrium for the adsorption of *p*-hydroxy benzoate onto hematite surfaces was attained at 70 h, whereas it was 30 h for phthalate–hematite system. None of the three kinetics models (Bajpai, pseudo first order and pseudo second order) is applicable in the entire experimental time period; however, the pseudo second order kinetics model is considered to be better than the pseudo first order kinetics model in estimating the equilibrium concentration both the *p*-hydroxy benzoate–hematite and phthalate–hematite systems. The variation of adsorption density of *p*-hydroxy benzoate and phthalate onto hematite surfaces as a function of concentration of adsorbate was studied over pH range 5–9 at a constant ionic strength, $I = 5 \times 10^{-4}$ mol dm^{-3} and at constant temperature. The adsorption isotherms for both the systems were Langmuir in nature and the maximum adsorption density (Γ_{max}) of *p*-hydroxy benzoate is ~1.5 times more than that of phthalate on hematite at pH 5 and 30 °C in spite of an additional carboxylic group at ortho position in phthalate. This is due to the more surface area coverage by phthalate than that of *p*-hydroxy benzoate on hematite surface. The activation energy was calculated using Arrhenius equation and the activation energy for adsorption of *p*-hydroxy benzoate at hematite–electrolyte interface is ~1.8 times more than that of phthalate–hematite system. The negative Gibbs free energy indicates that the adsorption of *p*-hydroxy benzoate and phthalate on hematite surfaces is favourable. The FTIR spectra of *p*-hydroxy benzoate and phthalate after adsorption on hematite surfaces were recorded for obtaining the bonding properties of adsorbates. The phenolic ν_{C-O} appears at ~1271 cm^{-1} after adsorption of *p*-hydroxy benzoate on hematite surfaces, which shifted by 10 cm^{-1} to higher frequency region. The phenolic group is not deprotonated and is not participating in the surface complexation. The shifting of the ν_{as}(–COO$^-$) and ν_s(–COO$^-$) bands and non-dissolution of hematite suggest that the *p*-hydroxy benzoate and phthalate form outer-sphere surface complex with hematite surfaces in the pH range of 5–7.

Keywords: Adsorption; *p*-Hydroxy benzoate; Phthalate; Hematite; FTIR; Kinetics

1. Introduction

The adsorption studies of benzenecarboxylic acid at the metal oxide– and (oxy)hydroxide–water interface have attracted much attention due to its goechemical, environmental and industrial importance. The position of an additional –COOH or –OH functional group or both in the benzenecarboxylic acid significantly influences the adsorption behaviour on the metal oxide surfaces in aqueous medium. Gu et al. [1] and Evanko and Dzombak [2,3] studied the adsorption behaviour of benzenecarboxylic acids on metal oxide surfaces and suggested possible surface complexation through carboxylic and phenolic groups depending on the functionality and polydispersibility of the respective benzenecarboxylic acid. The results also showed that the extent of adsorption of benzenecarboxylic acids with different functionalities on goethite surfaces in aqueous medium was different. For example, the adsorption density of benzenecarboxylic acids adsorbed on goethite surfaces under similar experimental conditions are in the order of mellitic acid (benzene hexacarboxylic acid) > pyromellitic acid (benzene-1,2,4,5-tetracarboxylic acid) > trimellitic acid (benzene-1,2,4-tricarboxylic acid) > phthalic acid (benzene-1,2-dicarboxylic

* Corresponding author. Fax: +91 0 376 2370011.
E-mail address: mahirrljt@yahoo.com (S. Mahiuddin).

0021-9797/$ – see front matter
doi:10.1016/j.jcis.2006.10.049

acid) > benzoic acid (benzenecarboxylic acid) [2]. Similarly, adsorption of phthalate, salicylate and *p*-hydroxy benzoate on oxide surfaces showed that an adjacent –COOH group greatly influences the adsorption density than that of –OH group at ortho or para position [1]. Das and Mahiuddin [4] also reported higher adsorption density of benzenecarboxylate with an additional $–COO^-$ at ortho position i.e. phthalate on α-alumina surfaces and was ∼5 times more than benzoate at pH 6.

Gu et al. [1] investigated the adsorption of humic acid on the iron oxide surfaces and reported that both carboxylic and hydroxyl groups are involved in surface complexation with iron oxide surfaces. The adsorption behaviour of benzenecarboxylic acid having an additional carboxylic or phenolic groups or both on the metal oxide and oxy(hydroxy) surfaces also suggests that the carboxylic group is relatively more active for binding on the oxide surfaces at lower pH, whereas hydroxyl group is relatively more important at higher pH [3,5]. However, these adsorption studies were discussed without kinetics.

In the scope of adsorption studies, kinetics of adsorption is found to be an important parameter [4,6,7], which yields the equilibration time and is characteristic, not an arbitrary choice as found in the literature, for an adsorbate–adsorbent system in aqueous medium. The equilibration time is an essential parameter for subsequent adsorption isotherms.

The vibrational spectroscopy of the adsorbed benzenecarboxylic acids/anions on to oxide surfaces has attracted much attention in the literature. The binding mode of benzenecarboxylate on the metal oxide surfaces depends on the number and position of the functional groups, for example, the surface complexation of phthalate with the iron oxide and iron oxy(hydroxide) surfaces has been addressed by number of investigators using infrared spectroscopy [8–11]. Phthalate forms inner and/or outer sphere complexes with goethite surfaces [12] in contrast to inner-sphere surface complex with Fe(III)(aq) through only one carboxylic group [8]. On the other hand, *p*-hydroxy benzoate forms bidentate complexes with goethite surfaces and phenolic group has no role in complexation [8]. Recent FTIR studies suggest that the outer-sphere complexes of phthalate on the metal oxide surfaces were found to be predominant at higher pH and lower ionic strength, while inner-sphere complexes are favoured only at lower pH and higher ionic strength [10,12,13].

Further, the rate constant of the adsorption of benzenecarboxylate on the metal oxide surface depends on the functionality of the adsorbate molecule. For example, the rate constant for adsorption of phthalate on α-alumina surfaces is ∼2 times more than that of benzoate on the same adsorbent [4]. Similarly, the rate constant for adsorption of salicylate on the natural hematite is ∼4 times greater than that of benzoate [6].

In this paper, a comparative adsorption kinetics at a fixed pH, adsorption isotherms at different pH values, influence of ionic strength on the adsorption and the mode of surface complexation of phthalate and *p*-hydroxy benzoate, which bears an additional –COOH and –OH group at ortho and para position, respectively, at hematite–electrolyte interface are discussed.

2. Materials and methods

2.1. Materials

Hematite (>99.7%, Aldrich, Germany) was used without further purification and was reactivated at ∼120 °C before use. *p*-Hydroxy benzoic acid (>99.5%, E. Merck, India), phthalic acid (>99.5%, E. Merck, India), sodium hydroxide (>99.0%, s.d. fine-chem, India), sodium chloride (AR grade, E. Merck, India) and hydrochloric acid (AR grade, NICE Chemicals, India) were used without further purification. *p*-Hydroxy benzoate and disodium phthalate were prepared from the reaction of respective acids with sodium hydroxide maintaining pH 6 and 7.3, respectively.

2.2. Adsorbent

Fourier transform infrared (FTIR) (Model-2000, Perkin-Elmer, USA) spectra, X-ray diffraction (XRD) (JDX11P3A, JEOL, Japan) and differential thermal analysis (DTA) and thermogravimetric analysis (TGA) (SDT 2960, TA Corporation, USA) of hematite were recorded. The surface area of hematite was determined by BET method and was found to be 4.88 $m^2\,g^{-1}$. The adsorption site concentration was determined by following the procedure of Hohl and Stumm [14] and was found to be TOT (≡FeOH) = 0.5166 $mol\,dm^{-3}$ based on the site density of 1.913 site nm^{-2}.

2.3. Adsorption kinetics

The adsorption density of *p*-hydroxy benzoate and phthalate separately on hematite (0.5 g) in a 15 mL suspension at pH 5 and ionic strength, $I = 5 \times 10^{-4}$ $mol\,dm^{-3}$ NaCl in a batch process was measured as a function of time at three different temperatures. The suspensions at different intervals of time were cooled and centrifuged at 12500 rpm for 15 min (relative centrifugal force = 28790 g). The residual concentration of *p*-hydroxy benzoate and phthalate was estimated at $\lambda_{max} = 246$ and 273 nm (absorption maximum), respectively with a UV–visible spectrophotometer, Specord 200 (Analytikjena, Germany). The amount of adsorbate adsorbed per unit surface area of the adsorbent (adsorption density) was estimated by mass balance using the following relation

$$\Gamma = (C_0 - C_e)V/ma, \tag{1}$$

where C_0 and C_e are the initial and residual concentration in $mol\,dm^{-3}$ of the adsorbate in the suspension, V is the volume of the suspension and m and a are the mass and surface area of the adsorbent, respectively.

2.4. Adsorption isotherms

Adsorption of *p*-hydroxy benzoate and phthalate on the hematite surfaces was carried out at 30 and 20 °C, respectively, in a screw-capped glass tube. A suspension of 15 mL containing 0.5 g hematite and 5×10^{-4} $mol\,dm^{-3}$ NaCl solution was mixed thoroughly with the help of a vortex mixer. The pH of the

suspension was adjusted to a desired value within ±0.1 unit using either NaOH or HCl solution and then allowed to equilibrate for 1 h. The required amount of *p*-hydroxy benzoate or phthalate was added and the pH of the suspension was readjusted, if necessary. The suspension was then allowed to equilibrate with intermittent mixing for 70 and 30 h (duration of equilibrium adsorption test for *p*-hydroxy benzoate and phthalate, respectively). After the equilibration time is attained, the suspension was then centrifuged and the residual concentration of *p*-hydroxy benzoate and phthalate was estimated as outlined in Section 2.3.

2.5. Dissolution of hematite

The influence of pH on the solubility of hematite in the presence of *p*-hydroxy benzoate and phthalate at a fixed ionic strength, $I = 5 \times 10^{-4}$ mol dm^{-3} NaCl and at 25 °C was studied. For the purpose, adsorption of *p*-hydroxy benzoate and phthalate at different pH was carried out up to the respective equilibration time as followed for adsorption isotherm. After the equilibration time, the suspension was centrifuged and the dissolved Fe^{3+} in the supernatant liquid was estimated by atomic absorption spectrophotometer (AAanalyst-100 Perkin-Elmer, USA) using iron flame and oxy-acetylene gases at a wavelength of 248.3 nm.

2.6. FTIR spectroscopy

For FTIR spectroscopic studies 0.5 g of the hematite was equilibrated with 5.3×10^{-3} mol dm^{-3} *p*-hydroxy benzoate and 1×10^{-3} mol dm^{-3} phthalate at a desired pH maintaining the ionic strength, $I = 5 \times 10^{-4}$ mol dm^{-3} NaCl following the same procedure adopted for adsorption isotherms. The suspension was centrifuged and the residue was washed with distilled water once, centrifuged and dried in a vacuum desiccator over fused calcium chloride. The pellets were prepared using 2 mg of the sample in 200 mg of spectrograde KBr. The FTIR spectra with 4 cm^{-1} resolutions were recorded with a Perkin-Elmer FTIR spectrophotometer, model 2000, using Spectrum 3.2 software. In the mid infrared region, assignment and identification of peaks after adsorption of *p*-hydroxy benzoate and phthalate on hematite for symmetric and asymmetric –COO^- and C–C of aromatic ring vibrations are very difficult due to adsorption of water. Thus, in the present study, we subtracted the references FTIR spectra (hematite in KBr) from the spectra of the adsorbed *p*-hydroxy benzoate and phthalate using spectrum software.

3. Results and discussion

3.1. Adsorbent

The FTIR spectra show a broad band at 3455 cm^{-1} corresponding to the surface hydroxyl group on the hematite surfaces. The two bands at 548 and 475 cm^{-1} represent the asymmetric and symmetric Fe–O stretching vibration [15]. The *d*-values from the XRD pattern of hematite were found at 3.681, 2.694, 2.511, 2.201, 1.836, 1.692, 1.597, 1.483 and 1.448 Å, which are in excellent agreement with the reported values [16]. The thermogram (DTA and TGA) of the hematite sample shows that there is a very negligible change (∼0.2%) in the weight at ∼400 °C. The results show that the adsorbent used for the adsorption studies contains purely hematite phase.

3.2. Kinetics of adsorption of p-hydroxy benzoate and phthalate

The variation of adsorption density of *p*-hydroxy benzoate and phthalate on hematite surfaces with time at pH 5, fixed ionic strength, $I = 5 \times 10^{-4}$ mol dm^{-3} and at three different temperatures is depicted in Figs. 1 and 2, respectively. The state of adsorption equilibrium for adsorption of *p*-hydroxy benzoate on hematite–water interface is attained at 70 h at 30 and 35 °C. But at 40 °C the adsorption density of *p*-hydroxy benzoate on hematite surfaces increases up to 20 h and then it becomes nearly constant with the elapse of time. In the case

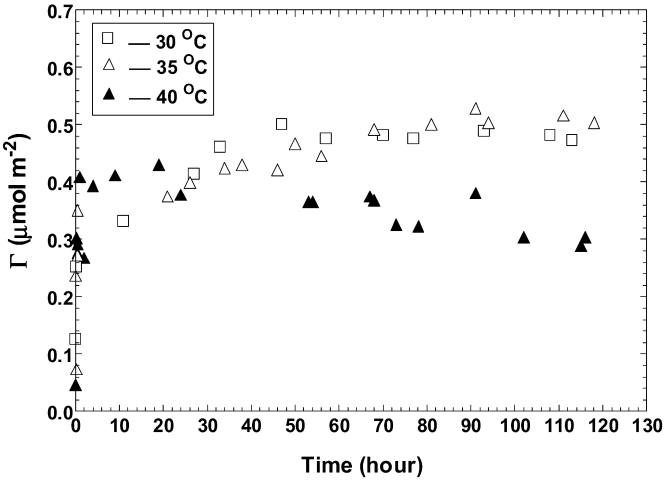

Fig. 1. Effect of temperature on the adsorption of *p*-hydroxy benzoate on hematite surfaces at fixed initial concentration of *p*-hydroxy benzoate: $C_0 = 5 \times 10^{-4}$ mol dm^{-3}, hematite = 0.5 g, $I = 5 \times 10^{-4}$ mol dm^{-3} NaCl, $V =$ 15 mL, pH 5.0.

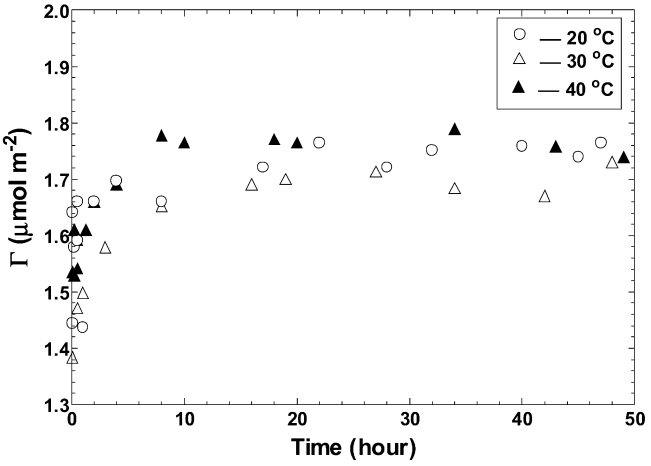

Fig. 2. Effect of temperature on the adsorption of phthalate on hematite surfaces at fixed initial concentration of phthalate: $C_0 = 5 \times 10^{-4}$ mol dm^{-3}, hematite = 0.5 g, $I = 5 \times 10^{-4}$ mol dm^{-3} NaCl, $V = 15$ mL, pH 5.0.

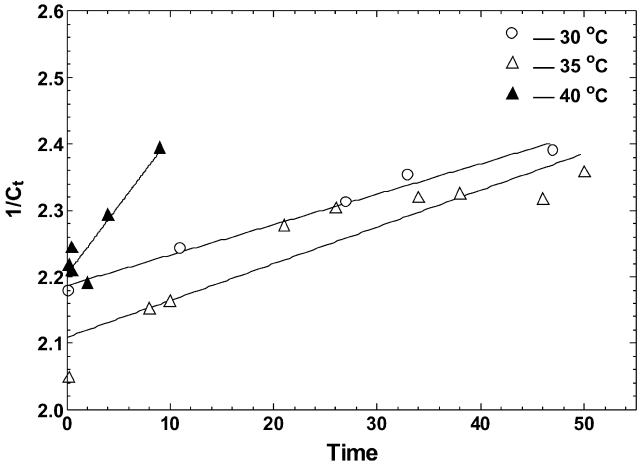

Fig. 3. Plot of $1/C_t$ versus time for the adsorption of p-hydroxy benzoate on the hematite surfaces at three different temperatures.

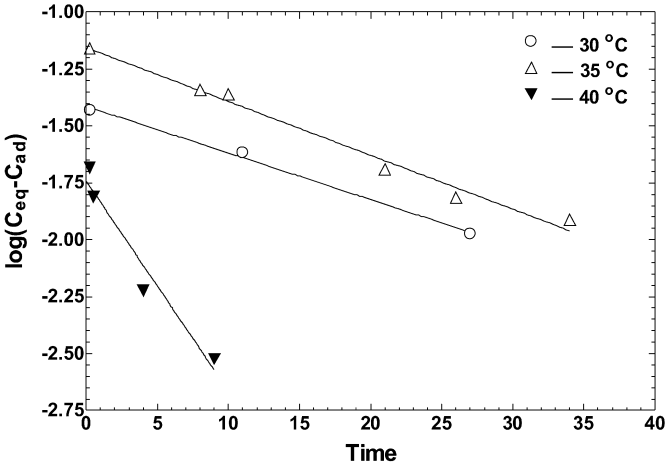

Fig. 5. Plot of $\log(C_{eq} - C_{ad})$ versus time for the adsorption of p-hydroxy benzoate on the hematite surfaces at three different temperatures.

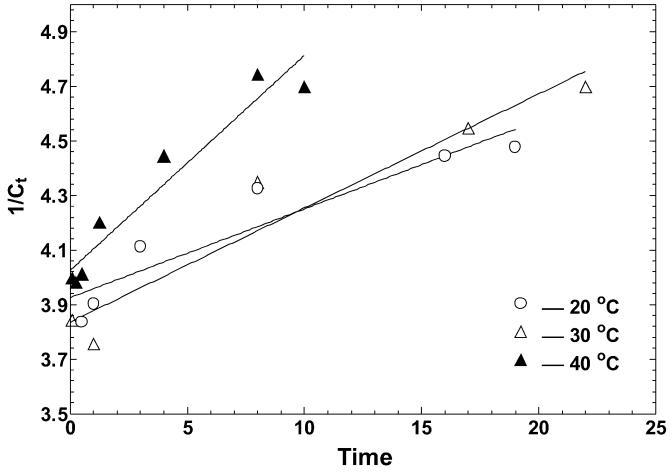

Fig. 4. Plot of $1/C_t$ versus time for the adsorption of phthalate on the hematite surfaces at three different temperatures.

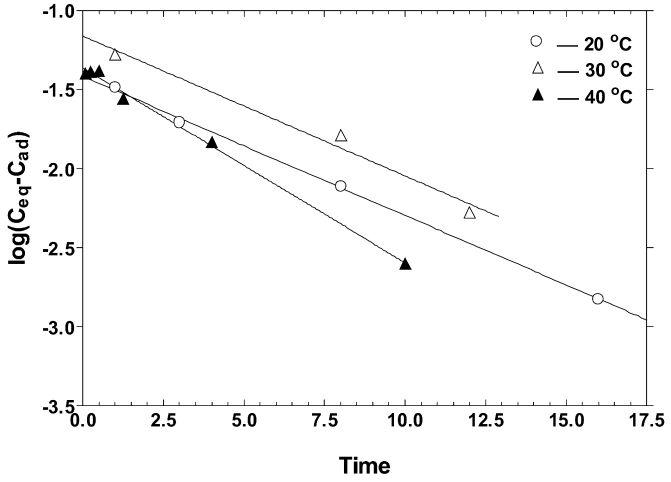

Fig. 6. Plot of $\log(C_{eq} - C_{ad})$ versus time for the adsorption of phthalate on the hematite surfaces at three different temperatures.

of phthalate–hematite system (Fig. 2) the state of adsorption equilibrium is attained at 30 h within the temperature range of study. The difference of the state of equilibrium for the p-hydroxy benzoate–hematite and phthalate–hematite systems is linked with the presence of different functional groups in two adsorbates. The presence of an additional –COOH group in ortho position in phthalate reduces the state of equilibrium time. An equilibration time, 70 and 30 h, was chosen for p-hydroxy benzoate– and phthalate–hematite system, respectively.

The kinetics parameter and the rate constant for adsorption, was estimated using the following kinetics models.

Bajpai [17] reported the following kinetics scheme based on the Langmuir adsorption isotherm equation:

$$1/C_t = k_1 t/C_0 + 1/C_0, \tag{2}$$

where C_0 and C_t are the initial and the residual concentration at time $t = 0$ and t, respectively, of the adsorbate, k_1 is the rate constant for adsorption. A plot of $1/C_t$ vs time is shown in Figs. 3 and 4 for p-hydroxy benzoate and phthalate, respectively at three different temperatures and the values of the fitted parameters are presented in Table 1 along with the normalised root-mean squares deviation. The rate constant for adsorption of p-hydroxy benzoate and phthalate on hematite surfaces increases with the increase in temperature and k_1 for phthalate–hematite system is ∼4–9 times more than that of p-hydroxy benzoate–hematite system.

For first order kinetics, simple Lagergren equation can be used to evaluate the rate constant for adsorption [18]

$$\ln(C_{eq} - C_{ad}) = \ln C_{eq} - k_2 t, \tag{3}$$

where C_{eq} and C_{ad} are the concentration of adsorbate adsorbed on oxide surfaces at equilibrium and at time t and k_2 is the pseudo first order adsorption rate constant. The plot of $\log(C_{eq} - C_{ad})$ vs t gives a straight line (Figs. 5 and 6) for p-hydroxy benzoate and phthalate, respectively and the rate constant can be obtained from the slope of the line and presented in Table 1. Generally, $\log C_{eq}$ (experimental value) is not equal to the intercept obtained from Eq. (3). This is the one of the major drawbacks of the pseudo first order kinetics model. The pseudo second order kinetics model (Eq. (4)) is also applicable for explaining the adsorption kinetics [19–21] and applied

Table 1
Values of the adsorption coefficient and the rate constants for p-hydroxy benzoate and phthalate adsorption on hematite surfaces

		p-Hydroxy benzoate			Phthalate		
		30 °C	35 °C	40 °C	20 °C	30 °C	40 °C
Bajpai kinetics model	k_1 (h^{-1})	2.29×10^{-3}	2.77×10^{-3}	1.03×10^{-2}	1.62×10^{-2}	2.09×10^{-2}	3.94×10^{-2}
	RMSD (ΔC_t (%))	0.48	1.77	1.95	2.35	2.72	1.97
Pseudo first order kinetics	k_2 (h^{-1})	0.0472	0.0545	0.2129	0.2025	0.2038	0.2833
	RMSD (ΔC_{ad} (%))	13.20	4.23	8.88	0.43	1.35	0.86
	C_{eq} (mmol dm^{-3})	0.0386	0.0703	0.0181	0.0383	0.0689	0.0432
Pseudo second order kinetics	k_3 (10^3 h^{-1} mol^{-1} dm^3)	1.0429	2.7115	40.7850	3.386	15.290	229.75
	RMSD (ΔC_{ad} (%))	18.24	31.42	27.95	9.64	32.28	5.81
	C_{eq} (mmol dm^{-3})	0.0972	0.0769	0.0687	0.2893	0.2868	0.2826
Experimental	C_{eq} (mmol dm^{-3})	0.0781	0.0813	0.07	0.2765	0.2863	0.2896
Adsorption coefficient	K_s	0.534	0.390	0.328	37.04	25.25	20.96

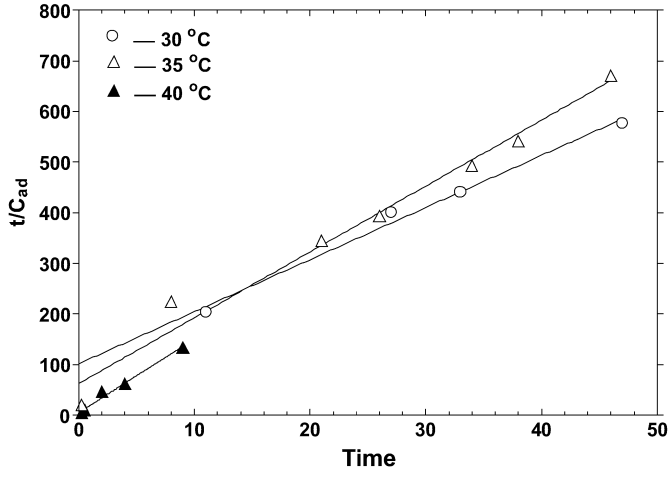

Fig. 7. Plot of t/C_{ad} versus time for the adsorption of p-hydroxy benzoate on the hematite surfaces at three different temperatures.

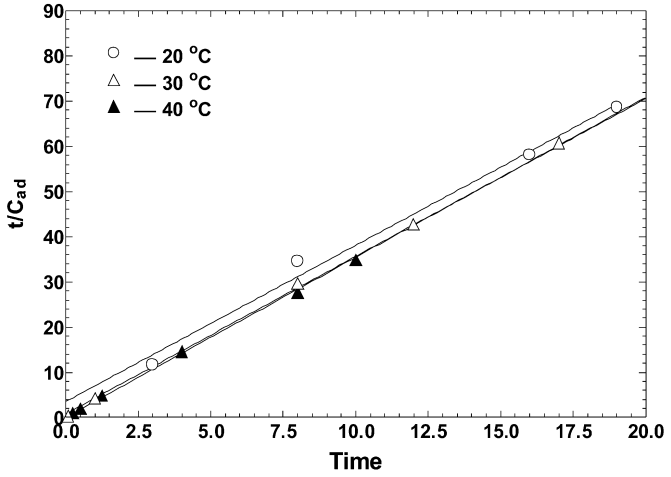

Fig. 8. Plot of t/C_{ad} versus time for the adsorption of phthalate on the hematite surfaces at three different temperatures.

to the present systems.

$$t/C_{ad} = 1/k_3 C_{eq}^2 + (1/C_{eq})t, \quad (4)$$

where C_{eq} and C_{ad} are the concentration of adsorbate adsorbed on oxide surfaces at equilibrium and at time t and k_3 is the second order rate constant. A plot of t/C_{ad} vs t gives straight line as shown in Figs. 7 and 8 for p-hydroxy benzoate and phthalate, respectively and the values of the fitted parameter are given in Table 1. The rate constant for adsorption k_3 for phthalate is ∼5–14 times greater than that of p-hydroxy benzoate at a fixed temperature. A similar variation of rate constant was observed for phthalate and benzoate adsorption at the α-alumina–water interface [4].

The calculated values of the C_{eq} parameter obtained from the pseudo first order kinetics model (Table 1) are not in agreement (13.50–74.18% and 75.93–86.1% deviation for p-hydroxy benzoate and phthalate, respectively) with that of experimentally obtained. This is one of the major discrepancies of the pseudo first order. The calculated values of the C_{eq} parameter from the pseudo second order kinetics models are in good agreement with experimentally obtained (1.8–24.45% and 0.17–4.6% deviation for p-hydroxy benzoate and phthalate, respectively). The results show that none of the three kinetics models is completely applicable in the entire time period of the kinetics run for both the systems. It seems that the Bajpai equation (Eq. (2)) is not applicable since it does not produce equilibration plateau. On the other hand, the pseudo first and second order models have application limitation at initial and final stage of the kinetics process [22]. Pseudo first order kinetics model fits the kinetics data better than the pseudo second order kinetics model in the initial stage of adsorption kinetics but higher deviation in the calculated equilibrium concentration was noted (Table 1), which is better reproduced by the pseudo second order kinetics model.

Adsorption of an adsorbate on an adsorbent is controlled by one or more steps, e.g., external diffusion, pore diffusion, surface diffusion and adsorption on pore surface or a combination of more than one step. The intra particle diffusion can be explained with the following equation [23,24].

$$C_{ad} = k_{id} t^{1/2}, \quad (5)$$

where k_{id} is the intra particle diffusion rate constant. A straight line of the plot of C_{ad} vs $t^{1/2}$ implies that the adsorption process is intra particle diffusion, but a multilinear plot suggests in-

Table 2
Values of the intra-particle diffusion and liquid film diffusion rate constants for *p*-hydroxy benzoate and phthalate adsorption on hematite surfaces

		p-Hydroxy benzoate			Phthalate		
		30 °C	35 °C	40 °C	20 °C	30 °C	40 °C
Intra-particle diffusion	k_{id} (10^{-3} mol dm^{-3} h$^{-0.5}$)	0.0097	0.0052	0.0082	0.0128	0.0152	0.0146
	R^2	0.992	0.991	0.927	0.924	0.953	0.942
	Intercepts	0.019	0.039	0.044	0.229	0.221	0.244
Liquid film diffusion	k_{fd} (h^{-1})	0.0472	0.0506	0.1856	0.2028	0.2039	0.2873
	R^2	0.996	0.976	0.967	0.999	0.979	0.996
	Intercepts	−0.704	−0.190	−1.547	−1.976	−1.424	−1.903

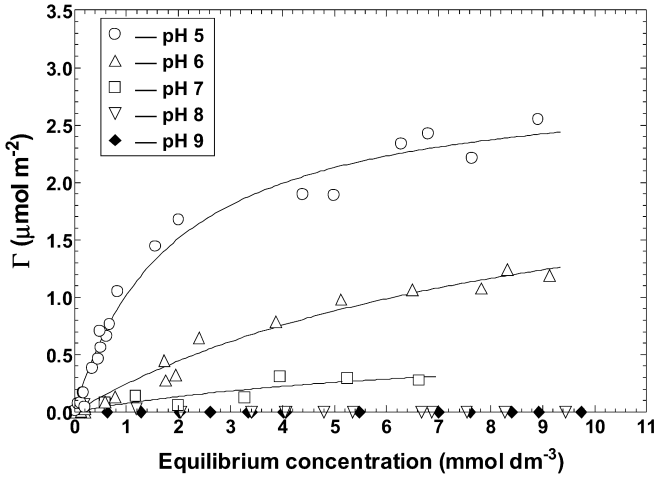

Fig. 9. Adsorption isotherms of *p*-hydroxy benzoate onto hematite at different pH, fixed $I = 5 \times 10^{-4}$ mol dm^{-3} NaCl, hematite = 0.5 g, $V = 15$ mL and at 30 °C. Symbols are experimental and the solid lines represent the theoretical value (Eq. (7)), respectively. The data points represent triplicate adsorption experiments.

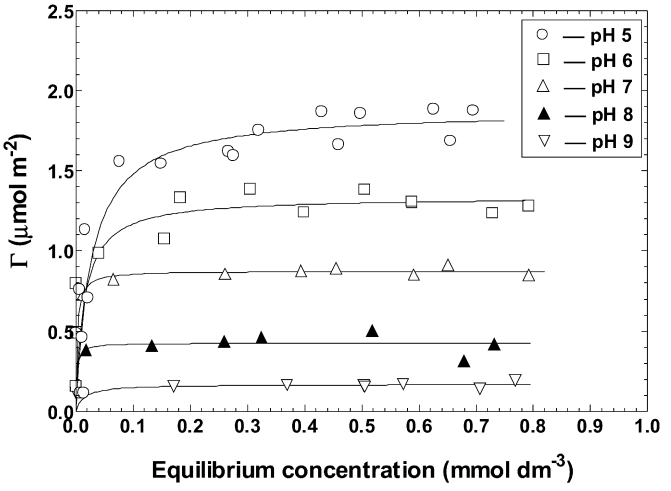

Fig. 10. Adsorption isotherms of phthalate onto hematite at different pH, fixed $I = 5 \times 10^{-4}$ mol dm^{-3} NaCl, hematite = 0.5 g, $V = 15$ mL and at 20 °C. Symbols are experimental and the solid lines represent the theoretical value (Eq. (7)), respectively. The data points represent triplicate adsorption experiments.

volvement of two or more steps in the adsorption process. The values of the parameter of Eq. (5) are given in Table 2.

The diffusion of adsorbate on the adsorbent surfaces can also be explained by the liquid film diffusion model [25]

$$\ln(1 - F) = -k_{fd}t, \tag{6}$$

where F is the fractional attainment of equilibrium ($F = C_{ad}/C_{eq}$) and k_{fd} is the adsorption rate constant. A linear plot of $-\ln(1 - F)$ vs t implies that the kinetics of adsorption process is controlled by diffusion.

The estimated value of the k_{id} and intercept is presented in Table 2. The nonzero value of intercept implies that the straight line is deviated from the origin for both the systems. This may be due to the difference in the rate of adsorption in the initial and final stage. Similarly, the nonzero intercept of Eq. (6) indicates that the liquid film diffusion model has limited application and none of the diffusion models is absolutely applicable due to heterogeneity of hematite.

3.3. Adsorption isotherms

The variation of adsorption density of *p*-hydroxy benzoate and phthalate at the hematite–electrolyte interface with different concentrations of adsorbate at a fixed ionic strength,

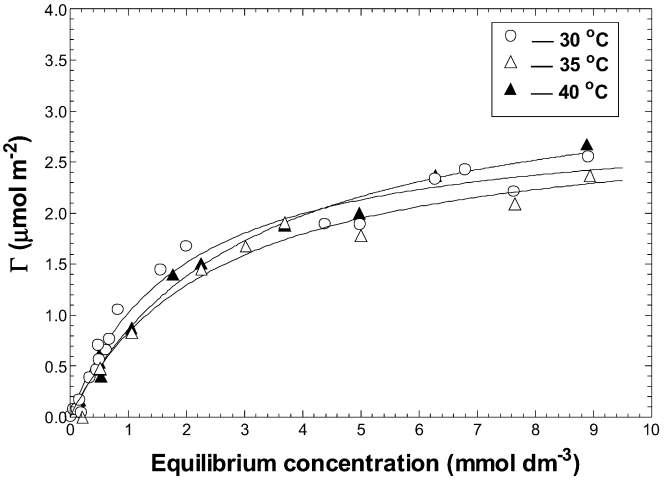

Fig. 11. Adsorption isotherm of *p*-hydroxy benzoate onto the hematite at 30 °C (○), 35 (△) and 40 °C (▲). Hematite = 0.5 g, $I = 5 \times 10^{-4}$ mol dm^{-3} NaCl, $V = 15$ mL, pH 5.

$I = 5 \times 10^{-4}$ mol dm^{-3} NaCl, different pH at 30 and 20 °C, respectively are Langmuir in nature (Figs. 9 and 10, respectively). Adsorption isotherms for both the systems at three different temperatures are also depicted in Figs. 11 and 12. The Langmuir adsorption isotherm equation of the following form was

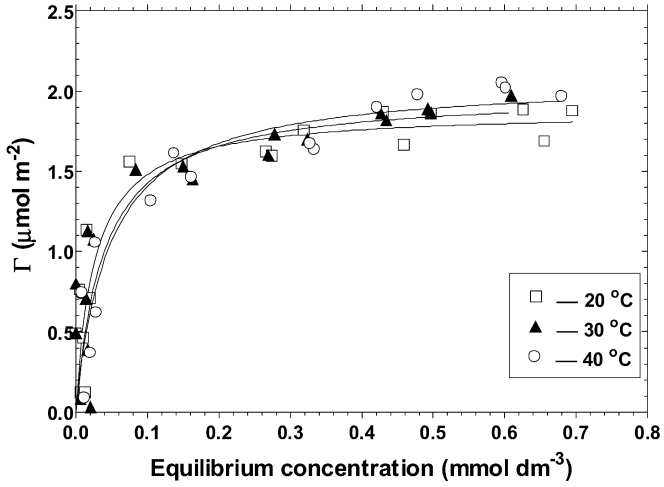

Fig. 12. Adsorption isotherm of phthalate on the hematite at 20 °C (□), 30 °C (▲) and 40 °C (○); hematite = 0.5 g, $I = 5 \times 10^{-4}$ mol dm^{-3} NaCl, $V = 15$ mL, pH 5.

Table 3
Values of the parameters of Langmuir equation (7) as function of pH for *p*-hydroxy benzoate and phthalate adsorption on hematite surfaces

Langmuir parameters	pH				
	5	6	7	8	9
p-Hydroxy benzoate					
Γ_{max} (μmol m^{-2})	2.927	2.523	0.654		
K_s	0.534	0.107	0.131		
Standard deviation	0.125	0.071	0.091		
Phthalate					
Γ_{max} (μmol m^{-2})	1.878	1.336	0.876	0.427	0.170
K_s	37.037	69.396	400.0	526.310	70.922
Standard deviation	0.243	0.353	0.221	0.075	0.046

used to fit the experimental adsorption data:

$$\Gamma = \Gamma_{max} C_e/(K + C_e), \quad (7)$$

where C_e is the equilibrium concentration of adsorbate in mmol dm^{-3}, $K = 1/K_s$, K_s is the adsorption coefficient and Γ and Γ_{max} are the concentration of the adsorbate in μmol m^{-2} at equilibrium and after saturation of the hematite surfaces, respectively. The value of Γ_{max} and K_s are presented in Table 3 and of the K_s at three different temperatures in Table 1. The adsorption density at saturation (Γ_{max}) of *p*-hydroxy benzoate onto hematite is ∼1.6 times more than that of phthalate at 30 °C and pH 5 in spite of the fact the phthalate has an additional –COOH group at ortho position, which enhances the adsorption density. The probable reason is due to the higher surface site coverage by phthalate than the *p*-hydroxy benzoate. Tejedor-Tejedor et al. [8] reported the Langmuir type adsorption isotherms for *p*-hydroxy benzoate and phthalate on goethite surface and the Γ_{max} of *p*-hydroxy benzoate is higher (∼1.6 times) in comparison to phthalate at 20 °C. Similarly, Γ_{max} for salicylate (with an additional –OH group at ortho position) on γ-Al_2O_3 surface at pH 4.3 is reported higher (∼1 mol kg^{-1}) than that of phthalate in spite of an additional –COOH group in the latter [5]. An alternative approach for finding the influence of –COOH over –OH group on adsorption is to consider isoequilibrium concentration for these systems at a particular temperature. In that case, the adsorption density, Γ of *p*-hydroxy benzoate and phthalate on the hematite surfaces at an equilibrium concentration of 0.5 mmol dm^{-3} is found to be 0.7 (Fig. 11) and 1.85 μmol dm^{-3} (Fig. 12), respectively at pH 5 and 30 °C. So, the presence of an adjacent –COOH group at ortho position in phthalate enhances the adsorption density on hematite surfaces than *p*-hydroxy benzoate under similar condition, is justified.

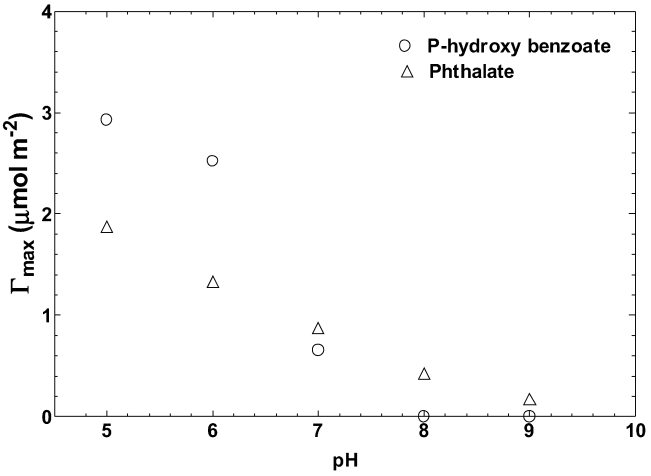

Fig. 13. Effect of pH on Γ_{max}.

The variation of Γ_{max} with pH for *p*-hydroxy benzoate– and phthalate–hematite systems is depicted in Fig. 13. The Γ_{max} of *p*-hydroxy benzoate and phthalate decreases with the increase in pH. In the case of *p*-hydroxy benzoate–hematite system, the adsorption density decreases up to pH 7 but no adsorption occurs at pH 8 and 9. The adsorption results (Fig. 13) imply that the $-COO^-$ in phthalate might be forming hydrogen bonding with surface hydroxyl groups of hematite whereas, for *p*-hydroxy benzoate, the adsorption density at pH 8 and beyond is zero as expected. The second carboxylic group of phthalate ionised at pH 7.3, which participates in the adsorption process by forming surface complexes with the hematite surfaces at pH 8 and 9. The results imply that the presence of adjacent –COOH group on phthalate exhibits the adsorption at pH 8 and 9 whereas –OH group in *p*-hydroxy benzoate does not participate in surface complexation on hematite surfaces at pH 8 and 9.

3.4. Variation of ionic strength

The variation of adsorption density of *p*-hydroxy benzoate and phthalate onto hematite surfaces with the increase in concentration of background electrolyte, NaCl at different pH and 30 and 20 °C, respectively is depicted in Figs. 14 and 15, respectively.

The adsorption density of *p*-hydroxy benzoate decrease linearly with the increase of ionic strength at pH 5 (Fig. 14). At pH 6, ionic strength has no influence on the adsorption of *p*-hydroxy benzoate. But at pH 7 adsorption of *p*-hydroxy benzoate on hematite surfaces is very small up to $I =$

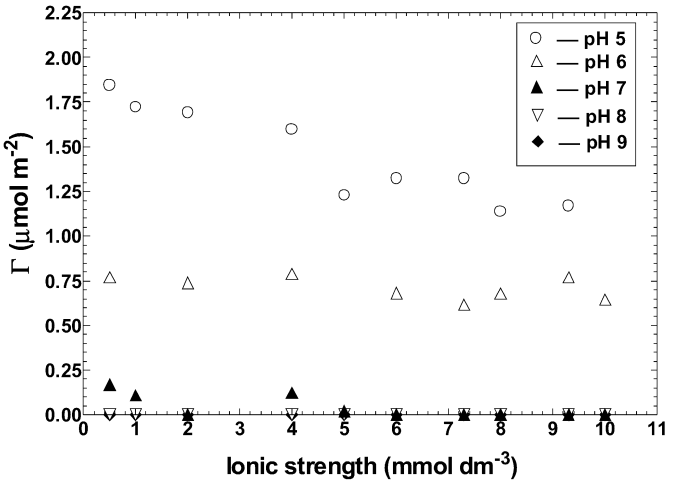

Fig. 14. Variation of adsorption density of p-hydroxy benzoate on hematite with ionic strength at different pH values and 30 °C, $C_0 = 5.3 \times 10^{-3}$ mol dm^{-3}, hematite = 0.5 g and $V = 15$ mL.

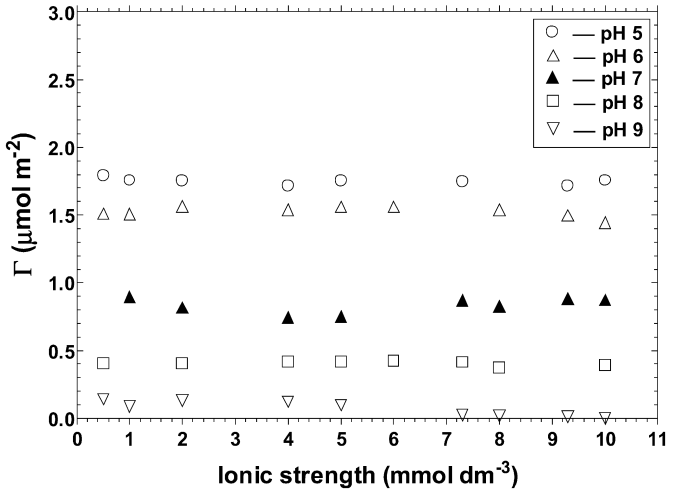

Fig. 15. Variation of adsorption density of phthalate on hematite with ionic strength at different pH values and 20 °C, $C_0 = 5 \times 10^{-4}$ mol dm^{-3}, hematite = 0.5 g and $V = 15$ mL.

~4 mmol dm^{-3} and beyond no adsorption is detected. It is evident that the adsorption of p-hydroxy benzoate on hematite surface is influenced by ionic strength only at pH = 5 of the medium. In phthalate–hematite system the ionic strength of the medium has, roughly, no influence on adsorption density. The influence of ionic strength on the adsorption of p-hydroxy benzoate on the hematite surfaces at pH 5 is due to increased distribution of chloride ion near the surface of hematite result in the decrease in thickness of the double layer [26].

3.5. Thermodynamic parameters

The activation energy for adsorption (E) of p-hydroxy benzoate and phthalate on hematite surface was estimated using Arrhenius equation, $k_3 = Ae^{-E/RT}$, where k_3 is the pseudo second rate constant for adsorption (Table 1), A is the frequency factor, R is the gas constant and T is temperature in Kelvin and the estimated values are listed in Table 4.

Table 4
Values of the thermodynamic parameters for adsorption of p-hydroxy benzoate and phthalate on hematite surfaces at pH 5

Temperature (K)	E (kJ mol^{-1})	ΔH (kJ mol^{-1})	ΔG (kJ mol^{-1})	ΔS (J mol^{-1} k^{-1})
p-Hydroxy benzoate				
303.15			−1.58	129.1
308.15	286.8	−40.7	−2.41	124.3
313.15			−2.90	120.7
Phthalate				
293.15			−8.81	44.9
303.15	161.2	−22.0	−8.14	45.6
313.15			−7.92	44.8

The Gibbs free energy (ΔG) of adsorption was estimated by the equation $\Delta G = -RT \ln K_s$, where K_s is the adsorption coefficient. The enthalpy (ΔH) value was obtained from the slope of the plot of $\ln K_s$ vs $1/T$ and entropy of the adsorption process was calculated by using the equation $\Delta G = \Delta H - T\Delta S$. It is apparent from Table 4 that the negative ΔH is an evident for the exothermic adsorption of p-hydroxy benzoate and phthalate on hematite surfaces. The activation energy for adsorption of p-hydroxy benzoate onto hematite surfaces is ~1.8 times higher than that of phthalate. The Gibbs free energy for both adsorbates is negative, which is more for phthalate–hematite. It is evident from the thermodynamic data that the adsorption of phthalate on hematite surfaces is more favourable than the p-hydroxy benzoate.

3.6. Dissolution of hematite surfaces

The concentration of Fe^{3+} in the supernatant liquid after treating with p-hydroxy benzoate and phthalate at two different concentrations as a function of pH is shown in Fig. 16. There is no detectable Fe^{3+} in the supernatant liquid in the pH range 4–9 with both p-hydroxy benzoate and phthalate. For p-hydroxy benzoate at pH 2 and 3 the concentration of Fe^{3+} are found to be 1.06 and 0.09 ppm at 0.01 mol dm^{-3} and 0.88 and 0.09 ppm at 5.3×10^{-3} mol dm^{-3}, respectively. On the other hand, the

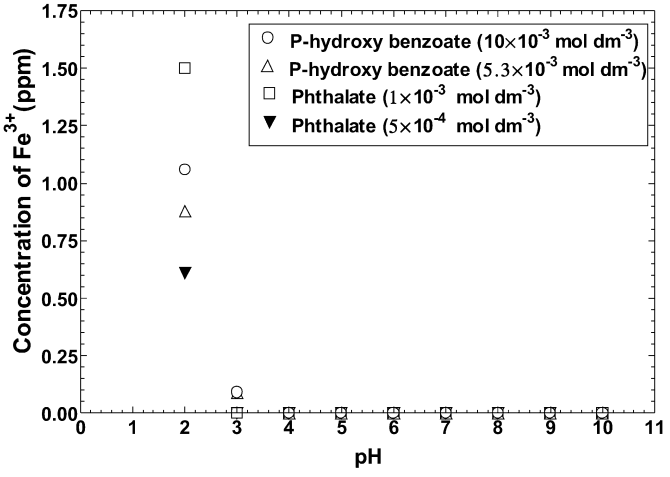

Fig. 16. Dissolution of hematite in presences of p-hydroxy benzoate and phthalate with pH at fixed ionic strength, $I = 5 \times 10^{-4}$ mol dm^{-3} and at 25 °C.

concentration of Fe^{3+} in the presence of 1×10^{-3} mol dm^{-3} and 5×10^{-4} mol dm^{-3} phthalate is found to be 1.50 and 0.61 ppm, respectively at pH 2. It is apparent from Fig. 16 that the dissolution of hematite increases with the increase of the concentration of *p*-hydroxy benzoate and phthalate at pH 5. Reported studies showed that the dissolution of minerals (aluminium and iron oxides and oxy (hydroxides)) was due to the formation of inner-sphere, bidentate, mononuclear complexes by low molecular weight organic acids/anions [27,28]. In the present study the absence of dissolution of hematite in presence of *p*-hydroxy benzoate and phthalate in the pH range 4–9 envisages the formation of outer-sphere complexes and will be discussed in the subsequent section.

3.7. FTIR spectra

The FTIR spectra of *p*-hydroxy benzoate and phthalate and their difference spectra after their adsorption on hematite surfaces at different pH are discussed in the subsequent section.

3.7.1. p-Hydroxy benzoate

The FTIR spectra of *p*-hydroxy benzoate (Fig. 17, inset) exhibit the peaks at 1542, 1416 and 1261 cm^{-1} (Table 5), which are assigned to ν_{as}(–COO$^-$), ν_s(–COO$^-$) and ν_{C-O} (between aromatic carbon and phenolic oxygen). The peak at 1611 cm^{-1} is assigned for ν_{C-C} (aromatic ring) and all peaks are in good agreement with the literature [29].

3.7.2. p-Hydroxy benzoate on hematite

The FTIR spectra of *p*-hydroxy benzoate after adsorption on the hematite surface at pH 5 and 7 are depicted in Fig. 17. The characteristic peak frequency of *p*-hydroxy benzoate and after adsorption on hematite surfaces are presented in Table 5. The characteristic band of ν_{as}(–COO$^-$) and ν_s(–COO$^-$) for the *p*-hydroxy benzoate after adsorption on the hematite surfaces

Table 5
Characteristic peak frequencies of *p*-hydroxy benzoate and after adsorption on hematite surfaces

Mode	ν (cm^{-1})		
	p-Hydroxy benzoate	pH 5	pH 7
ν_s(–COO$^-$)	1416	1408	1409
ν_{as}(–COO$^-$)	1542	1507	1506
ν_{C-C}(ring)	1611	1604	1600
ν_{C-O}(>C–OH)	1261	1271	1273

are found at 1507 and 1408 cm^{-1} and 1506 and 1409 cm^{-1} at pH 5 and 7, respectively. The peak at 1604 and 1600 cm^{-1} for pH 5 and 7, respectively, is assigned to ν_{C-C} (aromatic ring). The shifting of the peak frequency for ν_{C-C} by ∼7 cm^{-1} to lower frequency region w.r.t. 1611 cm^{-1} (ν_{C-C} (aromatic ring) for ligand) is due to the change of π electron density of *p*-hydroxy benzoate on adsorption on the hematite surfaces. The $\Delta\nu$ value ($\Delta\nu = \nu_{as} - \nu_s$ of –COO$^-$) is found to be ∼100 cm^{-1} at pH 5 and 7, respectively, which is ∼28 cm^{-1} smaller than the uncomplexed *p*-hydroxy benzoate.

Dobson and McQuillan [30] reported that the carboxylic group is co-ordinated by three different modes with metal oxide surfaces depending on the separation between the carboxylate asymmetric and symmetric stretching adsorption band ($\Delta\nu$). The band separation is generally taken for assigning different binding modes, e.g., 350–500 cm^{-1} for monodentate binding, 150–180 cm^{-1} for bridging and 60–100 cm^{-1} for chelating. So, the $\Delta\nu$ (∼100 cm^{-1}) suggests that the *p*-hydroxy benzoate should form a chelating bidentate surface complex with hematite surfaces at pH 5 and 7. On the contrary, taking $\Delta\nu$ as a tool for assigning surface complexation for benzenecarboxylate on metal oxide surfaces is being questioned [9]. *p*-Hydroxy benzoate forms a bidentate binuclear complexes with Fe(III) in solution, which is assigned considering the shifting of ν_s (–COO$^-$) band [8]. In the present system the phenolic ν_{C-O}

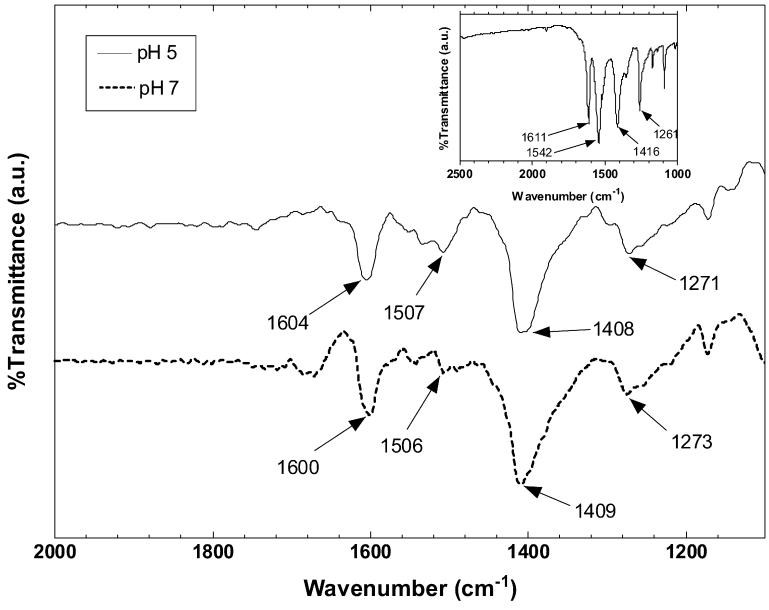

Fig. 17. FTIR difference spectra of *p*-hydroxy benzoate after adsorption on the hematite at two different pH values (Inset: FTIR spectra of *p*-hydroxy benzoate).

appears at 1271 and 1273 cm^{-1} at pH 5 and 7, respectively, which are resembled with the reported band frequency [8]. The small shifting of the band frequency ($\sim$10 cm^{-1}) of the phenolic stretching may be due to the co-ordination of *p*-hydroxy benzoate with hematite surface. Yost et al. [31] suggested that deprotonation of phenolic oxygen is possible if the shifting of ν_{C-O} is $\sim$30 cm^{-1} in the higher frequency range. Therefore, the hydroxyl group of *p*-hydroxy benzoate is not interacting with the hematite surfaces because of it unfavourable steric arrangement.

Further, $\nu_{as}(-COO^-)$ is shifted by $\sim$35 towards lower frequency region, which is accounted for the chemisorption of *p*-hydroxy benzoate on the hematite surfaces [30]. A similar complexation is evident from the shifting of $\nu_{as}(-COO^-)$ for salicylate adsorbed on goethite [32]. The shifting of $\nu_{as}(-COO^-)$ band and non-dissolution of hematite imply that *p*-hydroxy benzoate forms outer-sphere complexes with the hematite surfaces.

3.7.3. Phthalate

The FTIR spectra of phthalate (Fig. 18, inset) and the characteristic peak are presented in Table 6. The peaks at 1609, 1486 and 1441 cm^{-1} are due to ν_{C-C} (aromatic ring) vibrations. Two equivalent carboxylate groups are identified for two symmetric (ν_s) bands at 1388 and 1418 cm^{-1} and two asymmetric bands at 1552 and 1576 cm^{-1} [13]. The bands at 1085 and 1147 cm^{-1} are assigned for $\delta_{(C-H)}$. The band at $\sim$1704 cm^{-1} due to $\nu_{(C=O)}$ is absent for phthalate. But a small peak is observed at 1290 cm^{-1} for ν_{C-O}.

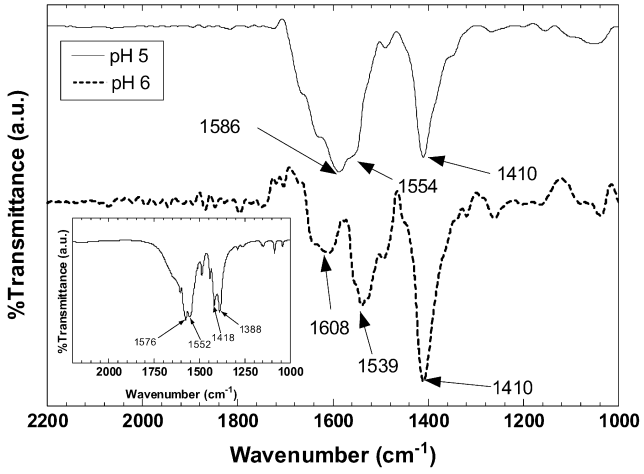

Fig. 18. FTIR difference spectra of phthalate after adsorption on the hematite at pH 5 and 6 (Inset: FTIR spectra of phthalate).

Table 6
Characteristic peak frequencies of phthalate and after adsorption on hematite surface

Mode	ν (cm^{-1})		
	Phthalate	pH 5	pH 6
$\nu_s(-COO^-)$	1388	1410	1410
	1418		
$\nu_{as}(-COO^-)$	1552	1554	1539
	1576	1586	
ν_{C-C}(ring)	1609		1608
	1486	1489	1495
	1441		1456

3.7.4. Phthalate on hematite

The FTIR spectra of phthalate after adsorption on the hematite surfaces at pH 5 and 6 are depicted in Fig. 18. The characteristic peak frequency of $\nu_{as}(-COO^-)$, $\nu_s(-COO^-)$ and ν_{C-C} (between aromatic ring and $-COO^-$) of phthalate after adsorption on hematite surface at pH 5 and 6 are presented in Table 6. The peak frequency of $\nu_{as}(-COO^-)$ and $\nu_s(-COO^-)$ after adsorption of phthalate on hematite surface appears at 1586 and 1410 cm^{-1} at pH 5 and 1539 and 1410 cm^{-1} at pH 6. The band at $\sim$1608, $\sim$1495, $\sim$1489, $\sim$1456 cm^{-1} are assigned for ν_{C-C} (ring).

The surface complexation of mono carboxylic acid with aqua metal ion can be assigned on the basis of difference between the asymmetric and symmetric stretching frequency ($\Delta\nu$) [8,31]. The mode of mixing between $-COO^-$ and aromatic ring vibration are highly probable in case of aromatic dicarboxylic acid. Moreover, the intramolecular vibrational interaction and the co-ordination will affect the splitting and position of $-COO^-$ band. Therefore, the magnitude of $\Delta\nu$ has not been considered in phthalate–hematite system for the identification of complexes for phthalate on hematite system.

Nordin et al. [13] proposed the outer- and inner-sphere surface complexes considering the shifting of $\nu_s(-COO^-)$ by $\sim$20 and $\sim$46 cm^{-1} to the high frequency region, respectively, and also the relative intensity change of symmetric band frequency in 1405 and 1422 cm^{-1} with increasing the ionic strength. It is reported data that inner-sphere complex is predominant at lower pH and higher ionic strength and the outer-sphere complex is favourable at higher pH and at lower ionic strength. In the present phthalate–hematite system the shifting of $\nu_s(-COO^-)$ is found to be $\sim$25 cm^{-1} at two pH, which favours the outer-sphere complexation. Johnson et al. [27] and Stumm [28] reported that the surface complexation formed by small organic anions on the oxide surfaces in an inner-sphere manner enhances the dissolution of oxide minerals. It is evident from the dissolution experiment in the present studies that there is no detectable Fe^{3+} in the supernatant liquid in the pH range 3–10. Therefore, based on the shifting of $\nu_s(-COO^-)$ and non-dissolution behaviour of hematite, phthalate forms outer-sphere complexes with hematite surfaces at pH 5 and 6.

4. Conclusions

With the above results following conclusions are drawn:

(1) The state of equilibrium in the case of *p*-hydroxy benzoate adsorbed on hematite surfaces at pH 5 in presence of 5×10^{-4} mol dm^{-3} NaCl is attained at 70 h, whereas, time required for the state of equilibrium for phthalate–hematite system under similar condition is 30 h at 30 °C. In the present system none of the three kinetics models (Bajpai,

pseudo first order and pseudo second order) is applicable in the entire experimental time period and temperature range.

(2) Adsorption density of *p*-hydroxy benzoate onto the hematite surfaces is ∼1.6 times more than that of phthalate at pH 5 and at 30 °C. The result is due to more surface site coverage by phthalate on hematite surface than of *p*-hydroxy benzoate.

(3) The maximum adsorption density, Γ_{max}, for *p*-hydroxy benzoate–hematite system decreases with the increase in pH and becomes zero at pH 8. In the case of phthalate–hematite system, Γ_{max} decreases up to the pH 9. The results are linked with ionisation of second and adjacent –COOH group, which participates in the adsorption by forming surface complexes with the hematite surfaces.

(4) The ionic strength has no influence on the adsorption of *p*-hydroxy benzoate and phthalate on hematite surface except at pH 5 for phthalate–hematite system.

(5) Activation energy for adsorption of phthalate on hematite is ∼ 1.8 times less than that of *p*-hydroxy benzoate–hematite system and the Gibbs free energy indicates that the adsorption of phthalate is more favourable on hematite than of *p*-hydroxy benzoate.

(6) The shifting of $\nu_{as}(–COO^-)$ and $\nu_s(–COO^-)$ after adsorption of *p*-hydroxy benzoate and phthalate and non-dissolution of hematite suggest that both *p*-hydroxy benzoate and phthalate form outer-sphere complexes with hematite surfaces in the pH range 5–7.

Acknowledgments

The authors are grateful to the Department of Science and Technology, New Delhi, India, for the financial support. The authors are also thankful to the Director, Regional Research Laboratory, Jorhat, India, for the facilities and interest in the work.

References

[1] B. Gu, J. Schmitt, Z. Chen, L. Liang, J.F. McCarthy, Geochim. Cosmochim. Acta 59 (1995) 219.
[2] C.R. Evanko, D.A. Dzombak, Environ. Sci. Technol. 32 (1998) 2846.
[3] C.R. Evanko, D.A. Dzombak, J. Colloid Interface Sci. 214 (1999) 189.
[4] M.R. Das, S. Mahiuddin, Colloids Surf. A. Physicochem. Eng. Aspects 264 (2005) 90.
[5] R. Kummert, W.J. Stumm, J. Colloid Interface Sci. 75 (1980) 373.
[6] M.R. Das, D. Bordoloi, P.C. Borthakur, S. Mahiuddin, Colloids Surf. A Physicochem. Eng. Aspects 254 (2005) 49.
[7] M.R. Das, O.P. Sahu, P.C. Borthakur, S. Mahiuddin, Colloids Surf. A Physicochem. Eng. Aspects 237 (2004) 23.
[8] M.I. Tejedor-Tejedor, E.C. Yost, M.A. Anderson, Langmuir 8 (1992) 525.
[9] N. Nilsson, P. Persson, L. Lövgren, S. Sjöberg, Geochim. Cosmochim. Acta 60 (1996) 4385.
[10] P. Persson, J. Nordin, J. Rosenqvist, L. Lövgren, L.-O. Öhman, S. Sjöberg, J. Colloid Interface Sci. 206 (1998) 252.
[11] J.-F. Boily, P. Persson, S. Sjöberg, Geochim. Cosmochim. Acta 64 (2000) 3453.
[12] O. Klug, W. Forsling, Langmuir 15 (1999) 6961.
[13] J. Nordin, P. Persson, E. Laiti, S. Sjöberg, Langmuir 13 (1997) 4085.
[14] H. Hohl, W. Stumm, J. Colloid Interface Sci. 55 (1976) 281.
[15] S. Subramanium, K.A. Natarajan, D.N. Sathyanarayana, Miner. Metall. Process 6 (1989) 152.
[16] M. King, W.F. McClune, H.E. Clark, B.L. Frank, T.M. Kahmer, L. Zwell, L.R. Bernstein, W.E. Mayo, H.F. McMurdie, F.J. Rotella, M.E. Mrose (Eds.), Powder Diffraction File, Alphabetic Index, Inorganic Phases, Sets 1–46, International Centre for Diffraction Data, Pennsylvania, USA, 1996.
[17] A.K. Bajpai, J. Appl. Polym. Sci. 51 (1994) 651.
[18] S. Lagergren, Ksver. Veterskapsakad. Handle 24 (1898) 1.
[19] C.T. Tien, C.P. Huang, Trace Metals in the Environmental, vol. 1, Heavy Metal in the Environment, Elsevier, Amsterdam, 1991.
[20] Y.S. Ho, G. McKay, Trans. IchemE. B 77 (1999) 165.
[21] Y.S. Ho, J.C.Y. Ng, G. McKay, Sep. Sci. Technol. 36 (2001) 241.
[22] F.-C. Wu, R.-L. Tseng, R.-S. Juang, Water Res. 35 (2001) 613.
[23] W.J. Weber, J.C. Morris, J. Sanit, Eng. Div. Am. Soc. Civ. Eng. 89 (1963) 31.
[24] Y.S. Ho, G. McKay, Trans. IchemE. B 76 (1998) 183.
[25] G.E. Boyd, A.M. Adamson, L.S. Myers, J. Am. Chem. Soc. 69 (1949) 2836.
[26] D.A. Dzombak, F.M.M. Morel, Surface Complexation Modelling: Hydrous Ferric Oxide, Wiley–Interscience, New York, 1990, chap. 9.
[27] S.B. Johnson, T.H. Yoon, B.D. Kocar, G.E. Brown Jr., Langmuir 20 (2004) 4996.
[28] W. Stumm, Colloids Surf. A Physicochem. Eng. Aspects 120 (1997) 143.
[29] M.I. Tejedor-Tejedor, E.C. Yost, M.A. Anderson, Langmuir 6 (1990) 979.
[30] K.D. Dobson, J. McQuillan, Spectrochim. Acta Part A 56 (2000) 557.
[31] E.C. Yost, M.I. Tejedor-Tejedor, M.A. Anderson, Environ. Sci. Technol. 24 (1990) 822.
[32] M.V. Biber, W. Stumm, Environ. Sci. Technol. 28 (1994) 763.